LANGMUIR Article
Cite This: Langmuir 2019, 35, 4860−4867
pubs.acs.org/Langmuir

Antibody-Oriented Strategy and Mechanism for the Preparation of Fluorescent Nanoprobes for Fast and Sensitive Immunodetection

Doudou Lou,[†] Lu Ji,[†] Lin Fan,[†] Yongxin Ji,[‡] Ning Gu,*[,†] and Yu Zhang*[,†]

[†]State Key Laboratory of Bioelectronics, Jiangsu Key Laboratory for Biomaterials and Devices, School of Biological Science and Medical Engineering & Collaborative Innovation Center of Suzhou Nano Science and Technology, Southeast University, Nanjing 210096, China

[‡]Nanjing Nanoeast Biotech Co., LTD, Nanjing 211100, China

Supporting Information

ABSTRACT: Nanoprobes have been widely used in biomedical engineering. However, antibodies are generally conjugated onto nanoparticles disorderly, which reduces their antigen recognition ability. The existing antibody orientation approaches are usually complex. Here, we developed and demonstrated a simple antibody-oriented strategy for the lateral flow immunoassay of cardiac troponin I by conjugating antibodies onto polystyrene nanospheres at the optimal pH. The binding amount and orientation of antibodies as well as the detection sensitivity were significantly improved. Although pH regulation is commonly used to optimize antibody conjugation, this paper illustrates the mechanism of its antibody orientation enhancement ability for the first time and reveals the important influences of the density, the charge distribution and hydrophilicity of the antibody, the control of the velocities of physical adsorption and chemical coupling, and other factors on antibody orientation. It is of great significance to understand and regulate antibody conjugation on the surface of micro- or nanospheres to construct high-performance probes for in vitro diagnosis applications.

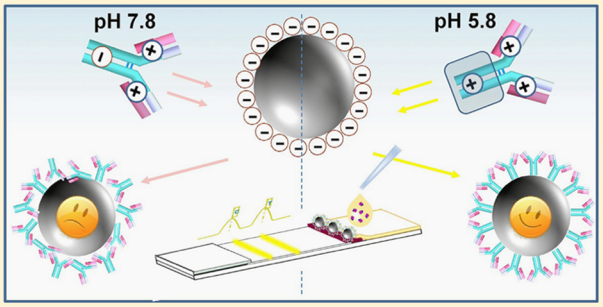

INTRODUCTION

Nanomaterials and nanoprobes play irreplaceable roles in the diagnosis of a range of diseases.[1,2] Owing to the demand of higher sensitivity, fluorescence, chemiluminescence, and electrochemiluminescence, immunoassays are gradually replacing conventional colloidal gold method and radioimmunoassay,[3−7] which have been widely used in the diagnosis and prognosis of diseases such as tumors, diabetes, and acute myocardial infarction.[8−10] For example, clinical biochemical analyzers usually employ streptavidin−biotin system to cross-link magnetic particles and antibodies, converting the concentration of antigen into chemiluminescence or electrochemiluminescence signals. Here, nanomaterials act as both protein carriers and signal amplifiers.[11] The immunoactivity of nanoprobes largely influences the detection sensitivity, which can be improved by regulating the surface properties of nanoparticles and increasing the loading capacity of antibodies.[12,13] Besides, the importance of antibody orientation has been realized.[14] Four major antibody orientations are "tail-on", "head-on", "side-on", and "flat-on".[15] Key approaches that have been proved to be effective are as follows: introducing crystalline fragment (Fc)-specific proteins such as protein A (or G); reducing antibodies to obtain thiol groups that anchor firmly on gold surfaces; oxidizing sugar chains of antibodies to obtain aldehyde groups that cross-link with hydrazine surfaces; fusion protein technology; and photo-cross-linking.[16−21] However, the above approaches are not only complicated but also have risks of decreasing antibody activity.

To find simpler methods for antibody orientation, the properties of antibodies such as charge distribution and hydrophilicity were considered.[22] The adsorption of antibodies onto nanoparticles is based on noncovalent forces,[23,24] which is not good for the repeatability, bonding strength, and stability. However, the results of adsorption can be easily regulated by changing the reaction environments. Emaminejad et al. treated antibodies as electric dipoles and applied lateral electric field to orient them, which led to more than 100% signal-to-noise enhancement.[25] It is effective to orient antibodies using external electric field on two-dimensional surfaces, but the approach is not suitable for nanoparticles. However, for surface-charged nanoparticles, every single particle is homogeneously covered by charged groups, and thus the surrounding microenvironment can be regarded as a miniature electric field, which, in turn, affects the interaction between antibodies and nanoparticles. For example, Puertas et al. oriented antibodies on magnetic nanoparticles and carbon nanotube-polystyrenes through an ionic or hydrophobic adsorption step before covalent cross-linking.[26] They stated that the conjugation process included an initial pre-adsorption followed by the

Received: January 15, 2019
Revised: February 27, 2019
Published: March 1, 2019

DOI: 10.1021/acs.langmuir.9b00150
Langmuir 2019, 35, 4860−4867

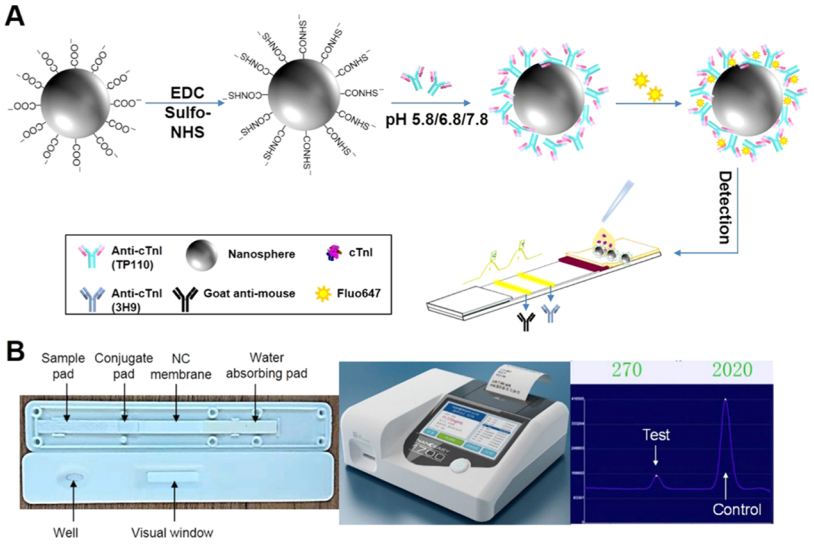

Figure 1. (A) Schematic representation of the preparation of antibody-modified nanoprobes involved in the lateral flow immunoassay. (B) The structure of the test strip (left), the fluorescent quantitative immunoassay analyzer (middle), and the data analysis interface on the computer (right).

formation of covalent bonds. In some of the research investigations, the mechanism of orientation is simplified such that the positively charged surfaces bind carboxyl groups at the C-terminal of antibodies and negatively charged surfaces bind amino groups at the N-terminal.[27,28] However, acidic and alkaline amino acids spread all over the whole antibody heterogeneously decide the charge distribution of antibodies and play important roles in the physical adsorption as well as provide binding sites for the cross-linking of chemical agents. It is to be noted that the final orientation of the antibodies is affected by various factors. In this study, antibody-oriented nanoprobes with higher immunoactivity were generated by a simple regulation of fewer reaction conditions. Besides, the mechanism of the influence of noncovalent interactions on antibody orientation was discussed.

Despite innumerous studies that reported on antibody orientation, there is still lack of maturity and methods of universal characterization. Technologies such as time-of-flight secondary ion mass spectrometry and spectroscopic ellipsometry show high resolution with reliable data and are thus frequently used to infer the direction of antibodies via measuring the changes of surface topography and thickness of protein layer.[29,30] However, these methods are more suitable only for two-dimensional materials compared to nanomaterials.[31] For nanoparticles, the characterization based on antigen−antibody binding seems to be more feasible and convincing, as it directly reflects the bioactivity of immobilized antibodies.[24] Antigens that can generate optical signals by themselves or through catalytic reactions are often employed to facilitate the detection and analysis; for instance, horseradish peroxidase can be used both as an antigen and a catalyst.[32] Even with a careful selection of model antigens and antibodies, the feasibility of the strategy of orientation does not completely reflect the clinical performance. In this study, cardiac troponin I (cTnI) was used to verify the practicality of the proposed method. As the gold standard for the in vitro diagnosis of acute myocardial infarction, the highly sensitive detection of cTnI is crucial for the exclusion and early diagnosis. Antibody orientation was determined using anti-mouse Fc antibodies (anti-Fc) and further confirmed by lateral flow immunoassay (LFIA), which is the most representative point-of-care testing method widely used in clinical diagnosis in recent years. There is a large market demand for LFIA because it is fast, cheap, and easy to operate. Its application in detecting low-concentration samples, however, has always been limited by low sensitivity. Antibody orientation is expected to improve the detection sensitivity of LFIA. The basic principles and processes of LFIA are shown in Figure S1. Figure 1A shows the preparation and steps in the immunoassay of nanoprobes, and Figure 1B indicates the structure of the test strip, the appearance of the detecting instrument, and the data analysis interface used in this study.

EXPERIMENTAL SECTION

Materials. The following reagents were used in the experiments: 240 nm-sized carboxylated polystyrene nanospheres (CNs) (JSR, Japan); bovine serum albumin (Yeasen, China); Alexa Fluor 647 *N*-hydroxysulfosuccinimide (NHS) ester (F647) (Thermo Fisher Scientific); *N*-(3-dimethylaminopropyl)-*N*′-ethylcarbodiimide hydrochloride crystalline (EDC); *N*-hydroxysulfosuccinimide sodium salt (sulfo-NHS), tris base, glycine (Sigma-Aldrich); human cardiac troponin I-T-C complex (Hytest, Finland); mouse anti-cTnI monoclonal antibodies (clone 3H9 and clone TP110) (OriGene, China), goat anti-mouse antibody, rabbit anti-mouse Fc antibody (anti-Fc) (Bioss, China); sample pad, conjugate pad, water-adsorbing pad, PVC plates (Kinbio, China); nitrocellulose membrane (NC membrane) (Merck, Germany); sucrose, sodium dodecyl sulfate (SDS) (Sinopharm, China); and 2-morpholineethanesulfonic acid (MES), Tween 20 and Triton X-100 (Biosharp, China).

Apparatus. The following are the main apparatus used in the experiments: A T-MS thermostatic oscillator (Topscien, China); a H1850R high speed centrifuge (Xiangyi, China); an ultraplus scanning electron microscope (SEM) (Zeiss, German); a UV1780 ultraviolet and visible spectrophotometer (Shimadzu, Japan); and a Nanoeasy1700 fluorescent quantitative immunoassay analyzer (Nanoeast, China).

Activation of Carboxylated Nanospheres. One milligram of 240 nm sized CNs was dispersed in 1 mL of 20 mM MES (pH 5.5) and incubated with 120 μg EDC and 120 μg sulfo-NHS at 37 °C for 40 min. Then, the mixture was centrifuged for 10 min at the speed of 20 000*g*. The obtained supernatant was discarded and the activated product was used immediately.

DOI: 10.1021/acs.langmuir.9b00150
Langmuir 2019, 35, 4860−4867

Details on Immobilization and Elution of TP110. *Immobilization of Clone TP110 at Different pH.* One milligram of activated product was resuspended in 350 μL of 10 mM phosphate buffer (pH 5.8, 6.8, or 7.8) and incubated with TP110 (50 or 200 μg) at 37 °C for 1 h. Then, the mixture was centrifuged for 10 min at the speed of 20 000*g*. The supernatant was collected and the CNs−TP110 conjugates were resuspended in 400 μL of 10 mM phosphate buffer (pH 6.8). The centrifugation steps were repeated twice and the products were stored at 4 °C until further use.

Immobilization and Elution of TP110 at Different Incubation Times. One milligrams of activated product was resuspended in 350 μL of 10 mM phosphate buffer (pH 5.8, 6.8, or 7.8) and incubated with 200 μg of TP110 at 37 °C for 5, 10, 20, 40, or 60 min. Then, the mixture was divided into two equal parts immediately. One part was centrifuged for 10 min at the speed of 20 000*g* and the supernatant was collected. Another part was incubated with 200 μL of SDS (2% w/v) in 100 mM of Tris (pH 7.5) at 37 °C for 30 min. It was then centrifuged for 10 min and the supernatant was collected. The SDS could fully elute the physically adsorbed antibodies without breaking any covalent bonds (Figure S2).

Specific Binding of Anti-Fc to TP110. A mixture of 200 μL of CNs−TP110 and 50 μg of anti-Fc was incubated at 25 °C for 15 min and centrifuged for 10 min at the speed of 20 000*g*, and the supernatant was collected.

Quantification of TP110 and Anti-Fc. Amounts of total binding, physical adsorption, and chemical cross-linking of TP110 as well as the binding amount of anti-Fc were all quantified by bicinchoninic acid protein quantitation kit. Each sample was diluted into 1 mL using pure water and incubated with 1 mL of working buffer at 60 °C for 60 min. The absorbance at 562 nm was then measured to determine the amount of protein based on the standard curves.

Conjugation of Fluorescent Molecules. Ten micrograms of F647 was incubated with 200 μL of CNs−TP110 at 25 °C for 60 min. Then, the mixture was purified by centrifuging three times. The nanoprobes were stored in 50 mM glycine buffer (pH 8.2) containing bovine serum albumin and sucrose as stabilizing agents at 4 °C until further use.

Preparation of Test Strips of Lateral Flow Immunoassay. Clone 3H9 was fixed in the test line area (2 mg/mL, 0.8 μL/cm) and goat anti-mouse antibody was fixed in the control line area (0.5 mg/mL, 0.8 μL/cm) of NC membrane. Nanoprobes were then evenly sprayed on the conjugate pad and air dried at 25 °C for 24 h. All membranes were then assembled orderly, cut into 4 mm wide test strips, and kept in plastic enclosures.

Procedure of Lateral Flow Immunoassay. One hundred microliters of cTnI sample was dropped onto the sample pad of a test strip. After 15 min, it was subjected to read by a fluorescent quantitative immunoassay analyzer. The performance of lateral flow immunoassay was then evaluated, which included linearity, repeatability, and limit of detection.

RESULTS AND DISCUSSION

Structural Characterization of Nanoprobes. Figure 2A shows the uniform dispersion of carboxylated polystyrene nanospheres (CNs). After conjugating with TP110, the size of CNs increased slightly. After Alexa Fluor 647 NHS ester (F647) labeling, a characteristic peak at 651 nm could be observed in the UV−vis absorption spectra (Figure 2B). Meanwhile, strong fluorescent signals were produced when the nanoprobes were dropped onto NC membrane and excited by light at 610 nm (Figure 2C).

Determination of Orientation of TP110 on Nanospheres. The isoelectric point (pI) of TP110 was about 6.8. To investigate the influences of pH on the adsorption, cross-linking, and orientation of antibodies, the reactions were carried out at pH 5.8, 6.8, and 7.8, which were below, equal to, and above the pI.

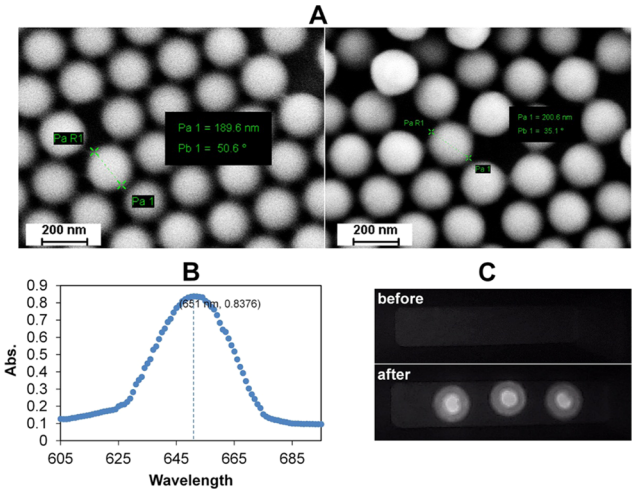

Figure 2. (A) SEM images of nanospheres before (left) and after (right) conjugating with antibodies. (B) UV−vis absorption spectra of nanoprobes. (C) Fluorescent signals of nanoprobes on the NC membrane.

TP110 Loading Capacity of CNs. As shown in Figure 3A, when the feeding amount of TP110 was low (50 μg), the binding amounts were high and almost the same at different pH. After increasing the feeding amount (200 μg), the binding amounts of antibody increased too. Obviously, a lower reaction pH led to a higher increase in the binding amounts of antibody. Hence, CNs had the maximum antibody loading capacity at pH 5.8.

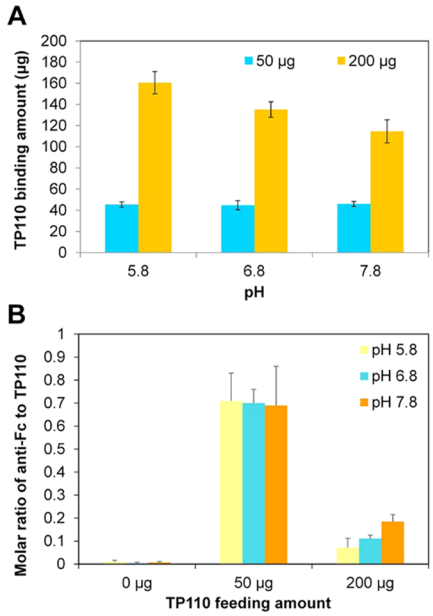

Figure 3. (A) Effect of pH and feeding amounts of TP110 on the binding amounts of TP110 on nanospheres. (B) Effect of pH and feeding amounts of TP110 on the molar ratio of anti-Fc to TP110.

Exposure of Fc Region of TP110. Anti-Fc specifically targeted the exposed Fc region of TP110. After it was incubated with CNs−TP110, the molar ratio of anti-Fc to TP110 was calculated. When the feeding amount of TP110 was 200 μg, less than one fifth of an anti-Fc was combined on each TP110. The lower the pH, the less the anti-Fc binding

DOI: 10.1021/acs.langmuir.9b00150
Langmuir 2019, 35, 4860−4867

amount, indicating that more Fc terminals of TP110 were toward the surface of CNs at pH 5.8 (Figure 3B). In other words, more antigen-binding fragments (Fab) were accessible for antigens. However, when the feeding amount of TP110 was 50 μg, the regularity was completely different. Nearly one anti-Fc was combined with each TP110, and the anti-Fc-to-TP110 ratio varied slightly with pH. The accessibility of the Fc region to TP110 was very similar, and thus the antibody orientations at different pH were unlikely to be determined only based on this experiment. Blank control (the feeding amount of TP110 was 0 μg) was also tested, which indicated that there was no nonspecific adsorption between anti-Fc and bare nanospheres.

Immunoactivity of Nanoprobes. The immunoactivities of nanoprobes prepared at different pH were examined with lateral flow immunoassay. Nanoprobes flow and react in the pores of NC membrane (Figure S3). For all groups, there was a positive correlation between the detection value and the concentration of cTnI (Figure 4A,B). The detection sensitivity

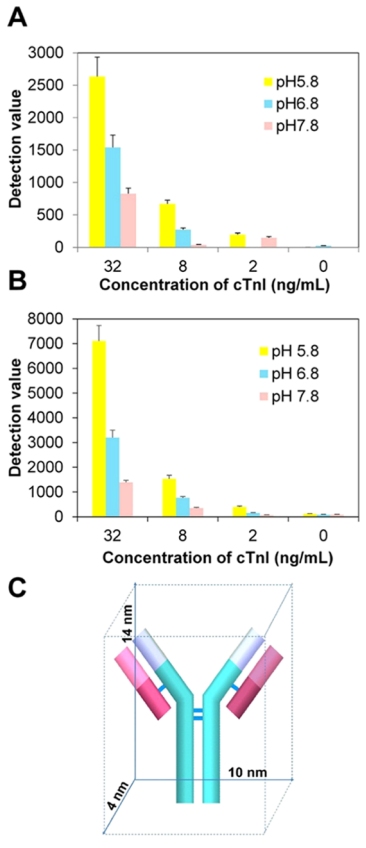

Figure 4. Lateral flow immunoassay results of cTnI using conjugates prepared with different feeding amounts of antibody: (A) 50 μg and (B) 200 μg. (C) The three dimensions of antibody.

increased as the pH decreased at both high (200 μg) and low (50 μg) feeding amounts of antibody. Since the same feeding amount of TP110 (200 μg) resulted in different binding amounts at different pH, and also had certain influence on the detection sensitivity, the feeding amount of TP110 was changed slightly (200 μg at pH 5.8, 240 μg at pH 6.8, and 280 μg at pH 7.8) to make the binding amount of TP110 uniform at different pH. The obtained results show that the detection sensitivity was still the highest at pH 5.8 (Figure S4).

It is to be noted that when the feeding amount of antibody was low (50 μg), the binding amounts of antibody and the degree of exposure of the Fc region at different pH were similar, but the antigen-binding activities of the Fab region were quite different, resulting in different sensitivities. Thus, TP110 orientation was the best at pH 5.8 in spite of the same exposure of the Fc region at pH 5.8, 6.8, and 7.8.

Determination of Total Binding, Physical Adsorption, and Chemical Cross-Linking Velocities of TP110. During the preparation of CNs−TP110 conjugates, first TP110 was physically adsorbed onto nanospheres followed by chemical cross-linking at the adsorption sites. Physical adsorption occurred rapidly, and thus the binding amounts of antibody at three pH were nearly saturated in 5 min (Figure 5A). However, with a decrease in the reaction pH, the cross-linking velocity of antibody was reduced (Figure 5B), since a higher protonation weakened the reactivity of amino groups. More than 96% of the adsorbed antibodies were cross-linked onto CNs at pH 7.8 in 5 min. At pH 5.8, the percentage was only 79. At pH 7.8, although the reaction of *N*-hydroxysulfosuccinimide sodium (sulfo-NHS) activated carboxyls with primary amines was highly efficient, the hydrolysis of sulfo-NHS ester was rapid too. The velocities of both cross-linking and hydrolysis decreased with a decrease in pH. As a result, at first, the window time between adsorption and cross-linking was prolonged, providing TP110 enough time to adjust the orientation under the influence of the microenvironment of the surface of nanosphere. Second, a slower hydrolysis ensures more activated carboxyl groups for the subsequent cross-linking reaction. Moreover, when the reaction pH was lower than pI, the net charge of the whole antibody was positive, opposed to negatively charged CNs, which also enhanced the electrostatic attraction and increased the binding amounts of antibody.

Effects of Density of Antibodies on the Performance of Nanoprobes. The density of antibodies on the surface of nanospheres affected steric hindrance, which is also critical for the orientation of antibodies.[33,34] At pH 5.8, when the feeding amount of TP110 was 50 μg, its binding amount was about 45.4 μg. Each antibody occupied an average area of 135 nm^2, which was about the area for one antibody lying in flat-on direction (Figure 4D). Therefore, during the preparation and preservation, the antibodies would turn spontaneously into a more stable state of low energy, and finally orient horizontally on the surface. When the feeding amount of TP110 was 200 μg, its binding amount was about 160.5 μg. Each antibody occupied an area of 40 nm^2, which was exactly for one antibody to immobilize in tail-on direction, indicating a compact and perpendicular arrangement of antibodies to the surface. This not only makes antibodies to be more in order and stable but also reduces nonspecific adsorption and misleading positive results caused by uncovered nanospheres or disordered distribution of protein. As a result, although a higher steric hindrance led to increased inactivation of antibody, the total number of immunoactive sites of probes was still larger and the detection sensitivity was higher than probes with low density of antibodies. When the reaction pH increased, the loading capacity of the antibodies of nanospheres decreased, which might be because the randomness of antibody orientation increased and each antibody required a large area on an average.

Based on the above results, in lateral flow immunoassay, optimized probes were used (the feeding amount of TP110 was 200 μg and the pH of conjugation was 5.8) to evaluate the performance. A good linear correlation between the concen-

DOI: 10.1021/acs.langmuir.9b00150
Langmuir 2019, 35, 4860−4867

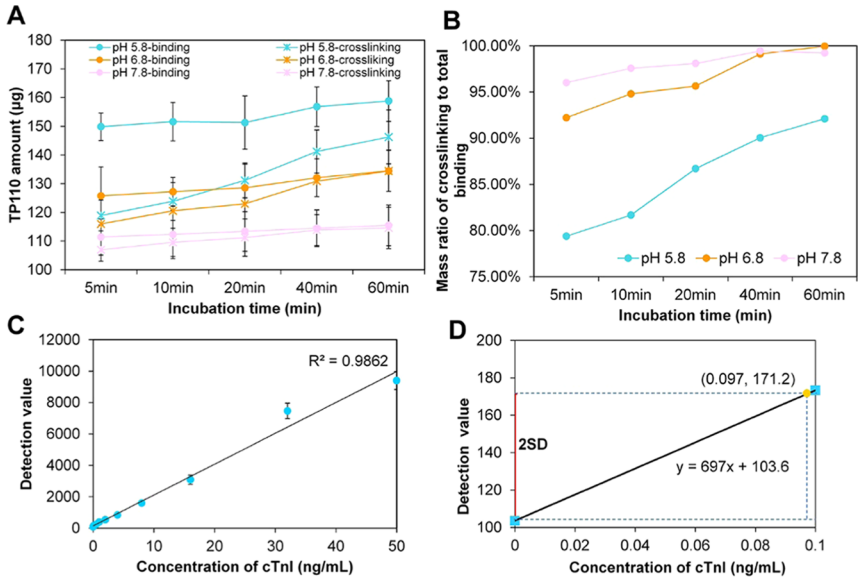

Figure 5. (A) Effect of incubation pH on the total binding (dots) and chemical cross-linking (asterisks) amounts of TP110 after conjugation for different time. (B) Effect of incubation pH on the mass ratio of chemical cross-linking of TP110 to the total binding of TP110. (C) Linearity of lateral flow immunoassay results of cTnI (0−50 ng/mL). (D) Limit of detection of lateral flow immunoassay.

tration of cTnI and the intensity of fluorescence within the tested concentration of 0.1−50 ng/mL could be noted (Figure 5C). Each of three representative concentrations of cTnI (0.5, 2, and 8 ng/mL) was tested 10 times and the calculated CV was 6.1, 8.0, and 9.7, respectively, showing a good reproducibility. A sample free from cTnI was tested 20 times, and the mean detection value (M) and standard deviation (SD) were calculated. The results of M + 2SD were lower than the mean detection value of 0.1 ng/mL of sample (mean of three replicates), thus the limit of detection was lower than 0.1 ng/mL (Figure 5D).

Discussion on the Mechanism of Orientation Based on the Physicochemical Properties of Antibodies. TP110 is one of the murine IgG1 monoclonal antibodies. There is only a small difference in the sequence of amido acid in the variable region among mouse IgG1 antibodies. The structure of a representative mouse IgG1 antibody (PDB ID: *1IGY*) was analyzed.[35] According to its charge distribution (Figure 6A), due to the existence of acidic and alkaline amino acids, as well as carboxyl and amino groups at the end of both heavy and light chains, positive and negative charges were unevenly distributed over the antibody, which determines the pI of whole antibody $(Fab)_2$ and Fc fragments. The pI of $(Fab)_2$ fragment was usually the largest and that of the Fc fragment the smallest,[16] differing by approximately 1−2. The number of alkaline amino acids was much more than acidic ones in the $(Fab)_2$ fragment, whereas the two were almost equal in the Fc fragment (Figure 6B). According to the Henderson−Hasselbalch equation, $pH = pK_a + lg([A^-]/[HA])$, the net charges of both $(Fab)_2$ and Fc fragments at different pH were calculated (Figure 6C). From pH 5.8 to 7.8, the absolute value of the net charge of the $(Fab)_2$ fragment was larger than that of the Fc fragment. Even when the net charge of the whole antibody was negative in an alkaline environment, the $(Fab)_2$ fragment was positively charged and affected the adsorption of antibody. Therefore, electrostatic attraction played a dominant role on the interaction between the positively charged $(Fab)_2$ fragment and the negatively charged nanosphere. In contrast, the Fc fragment was less charged and thus its hydration shell was thinner and hydrophobicity was stronger. At pH 7.8, both adsorption and cross-linking reactions were unfavorable for tail-on orientation of antibody. First, the $(Fab)_2$ fragment was positively charged, whereas the Fc fragment was negatively charged, so that the former was preferentially adsorbed onto nanospheres. Second, the deprotonation of the primary amino groups of Fab terminals was much more complete than that of lysine side chains and these primary amino groups were easier to be conjugated to carboxyl groups.

At pH 5.8, both the $(Fab)_2$ and Fc fragments were positively charged, thereby weakening the former's advantage of charge attraction. Also, most of the amino groups of Fab terminals were also protonated and thus their cross-linking priority was reduced. Besides, the hydrophobicity of the Fc region became stronger due to their rather small net charge, which more likely assisted in binding to nanospheres through hydrophobic interaction. Finally, the reduced cross-linking velocity provided a window time for the adsorbed antibodies to fully adjust their orientation before the formation of covalent bonds.

At pH 5.8−7.8, almost every carboxyl group on the surface of nanosphere was completely deprotonated and negatively charged. Compared with NHS, sulfo-NHS-activated nanospheres would not become neutralized, keeping the necessary surface charge density.[36]

In summary, the conjugation of CNs−TP110 began with physical adsorption under the influence of electrostatic and hydrophobic interactions. Essentially, the direction of antibodies was formed at this stage and then the covalent bonds were developed at the adsorbed sites. If the space between two antibodies was large enough, antibodies would continue to evolve into flat-on orientation. Finally, different amounts and orientations of antibodies were immobilized on nanospheres, which demonstrated different performances of anti-Fc and antigen recognition (Figure 7). In particular, when the feeding amount of TP110 was 50 μg, it was well oriented at pH 5.8 (Figure 7B) but random at pH 7.8 (Figure 7D), whereas the antibody densities were both low enough to fully expose the Fc region. This visually explains the results in Figures 3B and 4A

DOI: 10.1021/acs.langmuir.9b00150
Langmuir 2019, 35, 4860−4867

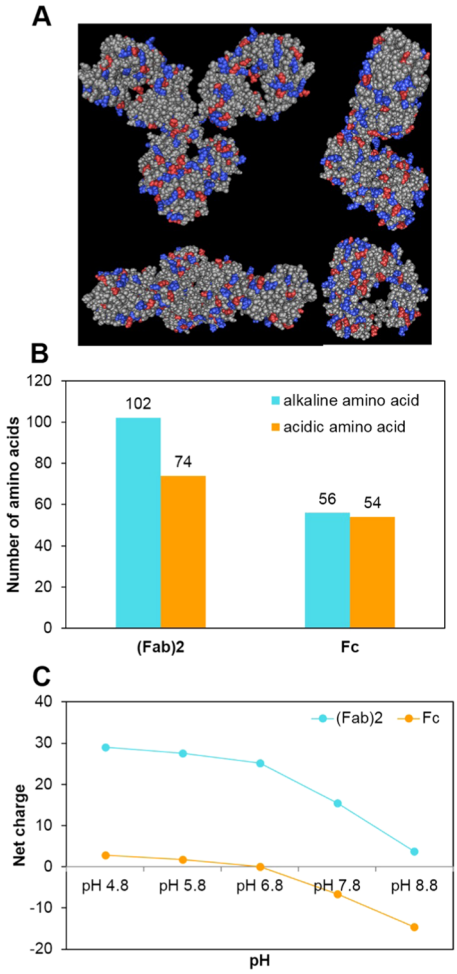

Figure 6. (A) Three-dimensional crystalline structure of IgG1 mouse monoclonal antibody (1IGY). Upper left: front view; upper right: lateral view; bottom left: top view; bottom right: bottom view. Alkaline and acidic amino acid groups have been marked with blue and red respectively. (B) Number of alkaline and acidic amino acids on $(Fab)_2$ and Fc fragments. (C) The net charge of $(Fab)_2$ and Fc fragments at different pH. The conserved sugar chains were ignored, so the charge distributions were not entirely consistent with the measured values of pI.

that the binding amounts of anti-Fc were similar but the detection sensitivities were different for these two probes.

CONCLUSIONS

To achieve better detection sensitivity, high-performance fluorescent nanoprobes were constructed by adjusting the conjugation pH of CNs−TP110. The mechanism of pH-induced antibody orientation and the effects of pH on the charge distribution, hydrophilicity, and adsorption/cross-linking velocity of antibodies were studied for the first time. When the pH reduced to 5.8, on the one hand, the distribution of charge and hydrophobic area of the antibodies facilitated their tail-on orientation, and on the other hand, the cross-linking velocity reduced, providing longer time for antibodies to fully adjust their direction under the influence of the microenvironment of the surface of nanospheres. Besides, the antibody-loading capacity of nanospheres significantly increased at pH 5.8. The density of antibody also had an important influence on the orientation of the final antibody. When the density was high enough, antibodies were closely aligned perpendicularly to the surface, which showed more order and stability. Probes were applied to the rapid detection of cTnI and the detection sensitivity was improved considerably. Overall, the optimized preparation strategy of probe that has been developed in this investigation is convenient and applicable to a wide range of antibodies and thus has potential application in in vitro diagnosis, especially for point-of-care testing.

ASSOCIATED CONTENT

Supporting Information

The Supporting Information is available free of charge on the ACS Publications website at DOI: 10.1021/acs.langmuir.9b00150.

Structure of test strips and the reaction process of lateral flow immunoassay, the SDS elution test results, SEM images of the NC membrane before and after the detection of cTnI positive sample, and the experimental results when the feeding amounts of TP110 were 200 μg at pH 5.8, 240 μg at pH 6.8, and 280 μg at pH 7.8 (PDF)

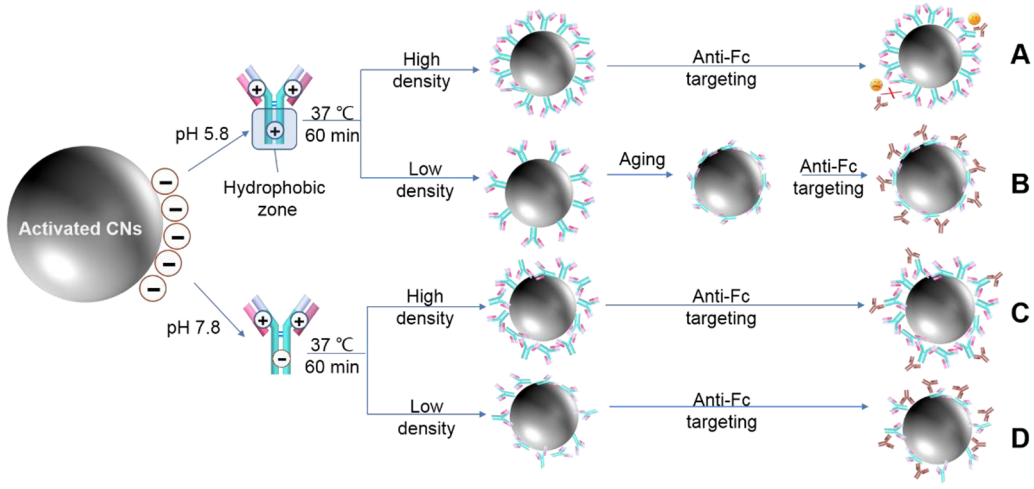

Figure 7. Random and oriented antibody immobilizations at different pH and antibody densities.

DOI: 10.1021/acs.langmuir.9b00150
Langmuir 2019, 35, 4860−4867

AUTHOR INFORMATION

Corresponding Authors

*E-mail: guning@seu.edu.cn (N.G.).
*E-mail: zhangyu@seu.edu.cn. Tel/Fax: +86 25 8327 2496 (Y.Z.).

ORCID

Ning Gu: 0000-0003-0047-337X
Yu Zhang: 0000-0002-0228-7979

Notes

The authors declare no competing financial interest.

ACKNOWLEDGMENTS

This work was supported by the National Key Research and Development Program of China [No. 2017YFA0205502]; National Natural Science Foundation of China [Nos 61821002, 81571806, and 81671820]; the Science and Technology Support Project of Jiangsu Province [No. BE2017763]; and the Fundamental Research Funds for the Central Universities. We also thank EditSprings for its linguistic assistance during the preparation of this manuscript.

REFERENCES

(1) Haun, J. B.; Devaraj, N. K.; Marinelli, B. S.; Lee, H.; Weissleder, R. Probing intracellular biomarkers and mediators of cell activation using nanosensors and bioorthogonal chemistry. *ACS Nano* **2011**, *5*, 3204−3213.

(2) Zhou, W.; Gao, X.; Liu, D.; Chen, X. Gold nanoparticles for in vitro diagnostics. *Chem. Rev.* **2015**, *115*, 10575−10636.

(3) Liu, X.; Niu, L.; Chen, Y.; Yang, Y.; Yang, Q. A multi-emissive fluorescent probe for the discrimination of glutathione and cysteine. *Biosens. Bioelectron.* **2017**, *90*, 403−409.

(4) Liu, Y.; de Keczer, S.; Alexander, S.; Pirio, M.; Davalian, D.; Kurn, N.; Ullman, E. F. Homogeneous, rapid luminescent oxygen channeling immunoassay (LOCI(TM)) for homocysteine. *Clin. Chem.* **2000**, *46*, 1506−1507.

(5) Liu, Q.; Ma, C.; Liu, X.; Wei, Y.; Mao, C.; Zhu, J. A novel electrochemiluminescence biosensor for the detection of microRNAs based on a DNA functionalized nitrogen doped carbon quantum dots as signal enhancers. *Biosens. Bioelectron.* **2017**, *92*, 273−279.

(6) Zhu, J.; Zou, N.; Zhu, D.; Wang, J.; Jin, Q.; Zhao, J.; Mao, H. Simultaneous detection of high-sensitivity cardiac troponin I and myoglobin by modified sandwich lateral flow immunoassay: proof of principle. *Clin. Chem.* **2011**, *57*, 1732−1738.

(7) Venge, P.; Roxin, L.; Olsson, I. Radioimmunoassay of human eosinophil cationic protein. *Br. J. Haematol.* **1977**, *37*, 331−335.

(8) Gao, M.; Yu, F.; Lv, C.; Choo, J.; Chen, L. Fluorescent chemical probes for accurate tumor diagnosis and targeting therapy. *Chem. Soc. Rev.* **2017**, *46*, 2237−2271.

(9) Bai, Y.; Gao, X.; Wang, Y.; Peng, X.; Chang, D.; Zheng, S.; Li, C.; Ju, S. Image-guided pro-angiogenic therapy in diabetic stroke mouse models using a multi-modal nanoprobe. *Theranostics* **2014**, *4*, 787−797.

(10) Cai, Y.; Kang, K.; Li, Q.; Wang, Y.; He, X. Rapid and sensitive detection of cardiac troponin I for point-of-care tests based on red fluorescent microspheres. *Molecules* **2018**, *23*, 1102−1114.

(11) Farka, Z.; Juřík, T.; Kovář, D.; Trnková, L.; Skládal, P. Nanoparticle-based immunochemical biosensors and assays: recent advances and challenges. *Chem. Rev.* **2017**, *117*, 9973−10042.

(12) Feng, B.; Huang, S.; Ge, F.; Luo, Y.; Jia, D.; Dai, Y. 3D antibody immobilization on a planar matrix surface. *Biosens. Bioelectron.* **2011**, *28*, 91−96.

(13) Liu, Y.; Zhang, Y.; Zhao, Y.; Yu, J. Phenylboronic acid polymer brush-enabled oriented and high density antibody immobilization for sensitive microarray immunoassay. *Colloids Surf., B* **2014**, *121*, 21−26.

(14) Shen, M.; Rusling, J.; Dixit, C. K. Site-selective orientated immobilization of antibodies and conjugates for immunodiagnostics development. *Methods* **2017**, *116*, 95−111.

(15) Trilling, A. K.; Beekwilder, J.; Zuilhof, H. Antibody orientation on biosensor surfaces: a minireview. *Analyst* **2013**, *138*, 1619−1627.

(16) Carrigan, S. D.; Scott, G.; Tabrizian, M. Real time QCM-D immunoassay through oriented antibody immobilization using cross-linked hydrogel biointerfaces. *Langmuir* **2005**, *21*, 5966−5973.

(17) Mazzucchelli, S.; Colombo, M.; De Palma, C.; Salvadè, A.; Verderio, P.; Coghi, M. D.; Clementi, E.; Tortora, P.; Corsi, F.; Prosperi, D. Single-domain protein A-engineered magnetic nanoparticles: toward a universal strategy to site-specific labeling of antibodies for targeted detection of tumor cells. *ACS Nano* **2010**, *4*, 5693−5702.

(18) Vikholm-Lundin, I.; Pulli, T.; Albers, W. M.; Tappura, K. A comparative evaluation of molecular recognition by monolayers composed of synthetic receptors or oriented antibodies. *Biosens. Bioelectron* **2008**, *24*, 1036−1038.

(19) Prieto-Simón, B.; Saint, C.; Voelcker, N. H. Electrochemical biosensors featuring oriented antibody immobilization via electrografted and self-assembled hydrazide chemistry. *Anal. Chem.* **2014**, *86*, 1422−1429.

(20) Seo, J. S.; Lee, S.; Poulter, C. D. Regioselective covalent immobilization of recombinant antibody-binding proteins A, G, and L for construction of antibody arrays. *J. Am. Chem. Soc.* **2013**, *135*, 8973−8980.

(21) Adak, A. K.; Li, B. Y.; Huang, L. D.; Lin, T. W.; Chang, T. C.; Hwang, K. C.; Lin, C. C. Fabrication of antibody microarrays by light-induced covalent and oriented immobilization. *ACS Appl. Mater. Interfaces* **2014**, *6*, 10452−10460.

(22) Wiseman, M. E.; Frank, C. W. Antibody adsorption and orientation on hydrophobic surfaces. *Langmuir* **2012**, *28*, 1765−1774.

(23) Zhou, J.; Tsao, H. K.; Sheng, Y. J.; Jiang, S. Monte carlo simulations of antibody adsorption and orientation on charged surfaces. *J. Chem. Phys.* **2004**, *121*, 1050−1057.

(24) Chen, S.; Liu, L.; Zhou, J.; Jiang, S. Controlling antibody orientation on charged self-assembled monolayers. *Langmuir* **2003**, *19*, 2859−2864.

(25) Emaminejad, S.; Javanmard, M.; Gupta, C.; Chang, S.; Davis, R. W.; Howe, R. T. Tunable control of antibody immobilization using electric field. *Proc. Natl. Acad. Sci. U.S.A.* **2015**, *112*, 1995−1999.

(26) Puertas, S.; de Gracia Villa, M.; Mendoza, E.; Jiménez-Jorquera, C.; de la Fuente, J. M.; Fernández-Sánchez, C.; Grazú, V. Improving immunosensor performance through oriented immobilization of antibodies on carbon nanotube composite surfaces. *Biosens. Bioelectron.* **2013**, *43*, 274−280.

(27) Ferreira, N. S.; Sales, M. G. Disposable immunosensor using a simple method for oriented antibody immobilization for label-free real-time detection of an oxidative stress biomarker implicated in cancer diseases. *Biosens. Bioelectron.* **2014**, *53*, 193−199.

(28) Sun, Y.; Du, H.; Feng, C.; Lan, Y. Oriented immobilization of antibody through carbodiimide reaction and controlling electric field. *J. Solid State Electrochem.* **2015**, *19*, 3035−3043.

(29) Liu, Y.; Yu, J. Oriented immobilization of proteins on solid supports for use in biosensors and biochips: a review. *Microchim. Acta* **2016**, *183*, 1−19.

(30) Welch, N. G.; Madiona, R. M. T.; Payten, T. B.; Easton, C. D.; Pontes-Braz, L.; Brack, N.; Scoble, J. A.; Muir, B. W.; Pigram, P. J. Surface immobilized antibody orientation determined using ToF-SIMS and multivariate analysis. *Acta Biomater.* **2017**, *55*, 172−182.

(31) Yuan, X.; Fabregat, D.; Yoshimoto, K.; Nagasaki, Y. Development of a high-performance immunolatex based on "soft landing" antibody immobilization mechanism. *Colloids Surf., B* **2012**, *99*, 45−52.

(32) Puertas, S.; Batalla, P.; Moros, M.; Polo, E.; Del Pino, P.; Guisan, J. M.; Grazú, V.; de la Fuente, J. M. Taking advantage of unspecific interactions to produce highly active magnetic nanoparticle-antibody conjugates. *ACS Nano* **2011**, *5*, 4521−4528.

DOI: 10.1021/acs.langmuir.9b00150
Langmuir 2019, 35, 4860−4867

(33) Batalla, P.; Bolívar, J. M.; Lopez-Gallego, F.; Guisan, J. M. Oriented covalent immobilization of antibodies onto heterofunctional agarose supports: a highly efficient immuno-affinity chromatography platform. *J. Chromatogr. A* **2012**, *1262*, 56−63.
(34) Zhao, X.; Pan, F.; Cowsill, B.; Lu, J. R.; et al. Interfacial immobilization of monoclonal antibody and detection of human prostate-specific antigen. *Langmuir* **2011**, *27*, 7654−7662.
(35) Harris, L. J.; Skaletsky, E.; Mcpherson, A. Crystallographic structure of an intact IgG1 monoclonal antibody. *J. Mol. Biol.* **1998**, *275*, 861−872.
(36) Pei, Z.; Anderson, H.; Myrskog, A.; Dunér, G.; Ingemarsson, B.; Aastrup, T. Optimizing immobilization on two-dimensional carboxyl surface: pH dependence of antibody orientation and antigen binding capacity. *Anal. Biochem.* **2010**, *398*, 161−168.

DOI: 10.1021/acs.langmuir.9b00150
Langmuir 2019, 35, 4860−4867